MOLECULAR AND CELLULAR BIOLOGY, Sept. 2004, p. 7829–7840 Vol. 24, No. 18
0270-7306/04/$08.00+0 DOI: 10.1128/MCB.24.18.7829–7840.2004

RhoE Inhibits Cell Cycle Progression and Ras-Induced Transformation

Priam Villalonga,[1] Rosa M. Guasch,[1]† Kirsi Riento,[1] and Anne J. Ridley[1,2]*

Ludwig Institute for Cancer Research, Royal Free and University College School of Medicine,[1] and Department of Biochemistry and Molecular Biology, University College London,[2] London, United Kingdom

Received 26 February 2004/Returned for modification 26 March 2004/Accepted 21 June 2004

Rho GTPases are major regulators of cytoskeletal dynamics, but they also affect cell proliferation, transformation, and oncogenesis. RhoE, a member of the Rnd subfamily that does not detectably hydrolyze GTP, inhibits RhoA/ROCK signaling to promote actin stress fiber and focal adhesion disassembly. We have generated fibroblasts with inducible RhoE expression to investigate the role of RhoE in cell proliferation. RhoE expression induced a loss of stress fibers and cell rounding, but these effects were only transient. RhoE induction inhibited cell proliferation and serum-induced S-phase entry. Neither ROCK nor RhoA inhibition accounted for this response. Consistent with its inhibitory effect on cell cycle progression, RhoE expression was induced by cisplatin, a DNA damage-inducing agent. RhoE-expressing cells failed to accumulate cyclin D1 or $p21^{cip1}$ protein or to activate E2F-regulated genes in response to serum, although ERK, PI3-K/Akt, FAK, Rac, and cyclin D1 transcription was activated normally. The expression of proteins that bypass the retinoblastoma (pRb) family cell cycle checkpoint, including human papillomavirus E7, adenovirus E1A, and cyclin E, rescued cell cycle progression in RhoE-expressing cells. RhoE also inhibited Ras- and Raf-induced fibroblast transformation. These results indicate that RhoE inhibits cell cycle progression upstream of the pRb checkpoint.

Rho GTPases are major regulators of cytoskeleton dynamics in eukaryotic cells and consequently have a crucial role in biological processes involving the cytoskeleton, such as the control of cell shape and motility (11). In mammalian cells, the best-characterized Rho family members are RhoA, Rac1, and Cdc42. Like other small GTPases, these proteins are molecular switches that, except for members of the Rnd subfamily (Rnd1, Rnd2, and RhoE/Rnd3) and RhoH/TTF, cycle between an active GTP-bound state and an inactive GDP-bound state. Once activated, they bind to and activate many downstream effectors, most of which are directly implicated in cytoskeletal regulation, leading to their characteristic effects, namely, the formation of actin stress fibers downstream of RhoA and the induction of actin-containing protrusions such as lamellipodia and membrane ruffles or filopodia downstream of Rac1 and Cdc42 (22, 32–34).

In addition to regulating cytoskeletal dynamics, Rho GTPases affect other cellular responses, such as transcriptional regulation, cell proliferation, and transformation (15, 40). The ectopic expression of activated mutants of RhoA, Rac1, and Cdc42 has been shown to promote cell cycle entry in quiescent fibroblasts, and the inhibition of their function with dominant-interfering mutants or inhibitors leads to cell cycle arrest (24, 50). Furthermore, activated mutants of these Rho GTPases positively contribute to cell transformation, and conversely, dominant-negative mutants have an inhibitory effect on Ras- and Raf-induced transformation (27–29). On the whole, the notion that Rho GTPases are positive regulators of both cell cycle progression and cell transformation is firmly established. However, little is known of the roles of different family members other than RhoA, Rac1, and Cdc42 in cell proliferation and transformation. A Rho family member that has attracted recent attention due to its atypical biochemical and functional properties is RhoE, a member of the Rnd subfamily of proteins that show no detectable GTPase activity and are thus constitutively bound to GTP (6). RhoE overexpression promotes the loss of actin stress fibers and focal adhesions together with an increase in cell migration via the inhibition of ROCK and/or the activation of p190RhoGAP (13, 35, 49). However, the possibility that RhoE affects other cellular responses regulated by Rho GTPases, such as the control of cell proliferation, has not been tested so far.

G_1 phase progression is driven by the sequential activation of cyclin-dependent kinases (cyclin D/cdk4 and cyclin E/cdk2) that takes place when cells receive the appropriate extracellular signals from both growth factors and the extracellular matrix (2). Under such conditions, D-type cyclins are synthesized in mid-G_1 phase (37), associating with cdk4, and the cyclin-dependent kinase inhibitor $p21^{cip1}$ is expressed at moderate levels. Active cdk4 promotes the phosphorylation and inactivation of the pocket proteins pRb, p107, and p130, allowing E2F transcription factors to induce the transcription of genes required for cell cycle progression, including cyclin E, which binds to and activates cdk2. In addition, cyclin D/cdk4 complexes enhance cyclin E/cdk2 activity by titrating out the cdk2 inhibitor $p27^{kip1}$ (44). Active cdk2 then phosphorylates $p27^{kip1}$ and triggers its degradation via the ubiquitin-proteasome pathway (47), further enhancing cdk2 activity and leading to pocket protein hyperphosphorylation and ultimately to passage through the G_1 restriction point.

Rho GTPases appear to contribute to G_1 progression mainly through cyclin D1 upregulation and through downregulation of the cdk inhibitor $p21^{cip1}$. Cyclin D1 expression can be regulated at multiple levels, including transcription, translation, and protein stability (9). Cyclin D1 transcription is affected by several transcription factors, including AP-1 and NF-κB, which

* Corresponding author. Mailing address: Ludwig Institute for Cancer Research, Royal Free and University College School of Medicine, 91 Riding House St., London W1W 7BS, United Kingdom. Phone: 44 20 7878 4033. Fax: 44 20 7878 4040. E-mail: anne@ludwig.ucl.ac.uk.

† Present address: Instituto de Investigaciones Citologicas (FVIB), 46010 Valencia, Spain.

can potentially be activated downstream of Rac and/or Cdc42 (4, 7), leading to cyclin D1 induction (16). Furthermore, RhoA/ROCK signaling regulates the timing of cyclin D1 expression in G_1 (48) through stress fiber-mediated integrin signaling that sustains ERK activation (36). In addition, Rac has been reported to mediate integrin-induced cyclin D1 translation (19). RhoA has also been shown to downregulate $p21^{cip1}$ under oncogenic stimulation (25), and accordingly, cell cycle arrest in response to RhoA inhibition is accompanied by an increase in $p21^{cip1}$ (17).

Here we show that RhoE can inhibit cell cycle progression in G_1. RhoE-mediated cell cycle arrest is characterized by a failure to translate cyclin D1. Interestingly, neither ROCK nor RhoA inhibition accounts for the cell cycle arrest elicited by RhoE, but the arrest can be rescued by the expression of proteins that bypass the pRb family pocket protein checkpoint, including human papillomavirus E7, adenovirus E1A, and cyclin E. We also show that RhoE can inhibit Ras- and Raf-induced transformation and that RhoE expression is induced by cisplatin, which induces DNA damage and pocket protein-dependent G_1 checkpoint arrest accompanied by a decrease in cyclin D1 expression. Our data indicate that RhoE has two functions, first to regulate the actin cytoskeleton and second to influence cell cycle progression.

MATERIALS AND METHODS

Cell culture. S2-6 cells are NIH 3T3 derivatives containing a tetracycline-inducible tTA transactivator, pTet-tTA (45), and they were kindly provided by David Schatz (Yale School of Medicine). S2-6 cells were grown in histidine-free Dulbecco's minimum essential medium (DMEM) supplemented with 10% donor calf serum, 0.5 μg of tetracycline/ml, and 0.5 mM histidinol (Sigma). NIH 3T3 cells were grown in DMEM supplemented with 10% donor calf serum. RhoE-3T3 cells were grown in histidine-free DMEM supplemented with 10% donor calf serum, 0.5 μg of tetracycline/ml, 0.5 mM histidinol, and 2 μg of puromycin (Sigma)/ml. Cells were made quiescent by culturing them for 24 h in medium containing 0.5% fetal bovine serum. Bromodeoxyuridine (BrdU), aLLnL, cycloheximide, cisplatin, daunorubicin, camptothecin (all from Sigma), and Y-27632 (Calbiochem) were added directly to the medium at indicated concentrations, and cells were harvested at the time points indicated in the figure legends.

Generation of RhoE-inducible cell lines. Threonine 37 of the mouse RhoE cDNA in pCMV5-Flag was mutagenized to asparagine by use of a QuikChange site-directed mutagenesis kit (Stratagene). The sequence changes were verified with an ABI Prism dye terminator cycle sequencing kit (Applied Biosystems). Wild-type and mutant (N37RhoE) mouse RhoE proteins were amplified from pCMV5-Flag-RhoE vectors by PCRs with the following oligonucleotides: forward, 5′-CCCAAGCTTTAAAGGAGAGAGCCAGC-3′, and reverse, 5′-GCT CTAGATCACATCACAGTACAGCTC-3′. The amplified sequence was then digested with HindIII and XbaI, and the resulting fragment was subcloned into the pTRE-HA vector (Clontech). pTRE-HA-RhoE constructs were cotransfected with pBabepuro into S2-6 cells. After puromycin (2 μg/ml) selection, individual puromycin-resistant clones were selected, amplified, and screened by Western blotting for inducible expression (with or without tetracycline) of hemagglutinin (HA)-RhoE by use of an anti-HA antibody (Covance Research). In addition, a dish of puromycin-resistant clones were pooled to create a population with inducible expression of HA-RhoE. Individual clones and the cell population are referred to collectively as RhoE-3T3 cells. Stable cell lines for Flag-RhoAV14, Flag-cyclin D1, cyclin D1-cdk4R24C, and E1A cells were generated by transfecting the indicated plasmids together with a hygromycin-resistant vector into RhoE-3T3 cells and following the same procedure as that outlined above.

Expression vectors and transient transfections. NIH 3T3 and RhoE-3T3 cells were transfected by using Lipofectamine 2000 (Invitrogen) according to the manufacturer's instructions with the following expression plasmids: cyclin D1 promoter-luciferase reporter (pGL3-1748CD1Luc; a gift of S. Cook), H-RasV12 (pcDNA3-H-RasV12; a gift of J. Downward), RafCAAX (pEF-mycRafCAAX; a gift of R. Marais), Flag-RhoE (pCMV5-Flag-RhoE [35]), Flag-RhoAV14 (pCMV5-Flag-RhoAV14; a gift of G. O. Cory), Flag-cyclin D1 (pCDNA3-Flag-cyclin D1; a gift of Carme Gallego), cyclin D1-cdk4R24C (pBabeDK; a gift of Parmjit Jat), cyclin E (pCMX-Myc-cyclin E; a gift of Roger Watson), E7 (pBabeE7; a gift of Parmjit Jat), E1A (pLPCE1A; a gift of Parmjit Jat), pEGFPC1 (Clontech), and an E2F-responsive luciferase reporter (pE2F-Luc; Clontech).

Gel electrophoresis and immunoblotting. Cells were harvested in a buffer containing 50 mM Tris-HCl (pH 7.4), 150 mM NaCl, 1 mM EDTA, and 1% (vol/vol) Triton X-100 plus protease and phosphatase inhibitors (2 μg of aprotinin/ml, 10 μg of leupeptin/ml, 1 mM phenylmethylsulfonyl fluoride, 1 mM dithiothreitol, 1 mM NaF, and 0.2 mM Na_3VO_4). Protein content was measured by the Bradford procedure, with bovine serum albumin as a standard (5). Cell lysates or proteins from pull-down or immunoprecipitation experiments were electrophoresed in sodium dodecyl sulfate (SDS)-polyacrylamide gels. After electrophoresis, the proteins were transferred to Immobilon P strips for 2 h at 60 V. The sheets were preincubated in a mixture of TBS (20 mM Tris-HCl [pH 7.5], 150 mM NaCl), 0.05% Tween 20, and 5% defatted milk powder for 1 h at room temperature and then were incubated for 1 h at room temperature in a mixture of TBS, 0.05% Tween 20, 1% bovine serum albumin, and 0.5% defatted milk powder containing the following antibodies, as appropriate: rabbit anti-phospho-ERK (9101; Cell Signaling) (1:1,000), anti-phospho-Akt (9271; Cell Signaling) (1:1,000), anti-p107 (sc-318; Santa Cruz) (1:1,000), anti-cyclin A (sc-596; Santa Cruz) (1:1,000), anti-$p27^{kip1}$ (sc-528; Santa Cruz) (1:1,000), anti-$p21^{cip1}$ (sc-471; Santa Cruz) (1:1,000), anti-cdk4 (sc-260; Santa Cruz) (1:1,000), anti-RhoE (35), anti-phospho-FoxO3a (06-952; Upstate Biotechnology) (1:1,000), and anti-phospho(Y397)-FAK (44-624; Biosource International) (1:1,000), antibodies; goat anti-cdk2 antibody (sc-163-G; Santa Cruz) (1:1,000); and mouse monoclonal anti-HA (MMS-101R; Covance Research) (1:1,000), anti-Rac1 (05-383; Upstate Biotechnology) (1:1,000), anti-cyclin D1 (sc-8396; Santa Cruz) (1:1,000), anti-RhoA (sc-418; Santa Cruz) (1:100), and anti-Flag (M2; Sigma) (1:1,000) antibodies. After being washed in TBS–0.05% Tween 20, the sheets were incubated with a peroxidase-coupled secondary antibody (1/2,000 dilution; Amersham) for 1 h at room temperature. After incubation, the sheets were washed twice in TBS–0.05% Tween 20 and once in TBS. The peroxidase reaction was visualized by ECL (Amersham).

Flow cytometric analyses and BrdU incorporation. Cell cycle profiles were measured by flow cytometry using propidium iodide. Briefly, trypsinized cells were collected by centrifugation, washed in phosphate-buffered saline, and fixed for 30 min at 4°C in 70% ethanol. After being washed twice with phosphate-buffered saline, DNAs were stained with propidium iodide (50 μg/ml) in the presence of 50 μg of RNase A (Sigma)/ml. Stained cells were then processed with a Becton Dickinson FACScan instrument and analyzed with Cell Quest software. For flow cytometric analysis of transiently transfected cells, cells were transfected with green fluorescent protein alone or together with the indicated vectors, and at 48 h posttransfection, the cells were harvested and incubated for 45 min at 37°C with 20 μg of Hoechst 33342 (Sigma)/ml. Green fluorescent protein-positive cells were then analyzed for DNA content with a UV laser (325 nm) in a Becton Dickinson LSR1 instrument and were analyzed with Cell Quest software. For analyses of S-phase entry, serum-starved or serum-stimulated cells were incubated with 3 μg of BrdU/ml for 2 h and then fixed in 3.7% formaldehyde for 15 min. Fixed cells were incubated for 1 h at 37°C with an anti-BrdU antibody (Amersham) and then for 45 min at 37°C with tetramethyl rhodamine isocyanate (TRITC)-conjugated goat anti-mouse immunoglobulin G (IgG) (Jackson Immunoresearch) (1:200).

Measurement of Rho and Rac activation. The capacities of Rho-GTP and Rac-GTP to bind to GST-rhotekin and GST-PBD (p21-activated kinase-binding domain), respectively, were used to analyze the amounts of active GTPases (31). Cells (5×10^6 to 10×10^6) were lysed with Rho/Rac extraction buffer (50 mM Tris-HCl [pH 7.5], 1 mM EDTA, 500 mM NaCl, 10 mM $MgCl_2$, 1% [vol/vol] Triton X-100, 0.5% sodium deoxycholate, 0.1% SDS, 10% [vol/vol] glycerol, 0.5% [vol/vol] 2-mercaptoethanol) plus the protease and phosphatase inhibitors described above. Cleared ($10{,}000 \times g$) lysates were incubated for 45 min at 4°C with glutathione-Sepharose 4B beads coupled to GST-rhotekin or GST-PBD (Upstate Biotechnology) for Rho-GTP or Rac-GTP pull-down assays, respectively. The beads were washed four times in extraction buffer. Bound proteins were solubilized by the addition of 35 μl of Laemmli loading buffer and were separated in SDS–12.5% polyacrylamide gels. The amount of Rho or Rac in the bound fraction was detected by Western blotting.

Immunofluorescence. Cells grown on coverslips were fixed in 3.7% (vol/vol) paraformaldehyde for 20 min and permeabilized in 0.2% (vol/vol) Triton X-100 for 5 min. Actin filaments were visualized by incubating the fixed cells for 45 min at 37°C with TRITC-phalloidin (Sigma) (1:500). For vinculin staining, cells were incubated for 1 h at 37°C with an antivinculin antibody (v-4505; Sigma) (1:200) followed by 1 h at 37°C with fluorescein-conjugated anti-mouse IgG (Jackson Immunoresearch) (1:200). For HA-RhoE staining, fixed cells were incubated for

1 h at 37°C with an anti-HA antibody (Covance) (1:400) followed by 1 h at 37°C with fluorescein-conjugated anti-mouse IgG (Jackson Immunoresearch) (1:200).

Northern blotting. Total RNAs were isolated from RhoE-3T3 cells by use of an RNeasy midikit (Qiagen) according to the manufacturer's instructions. The RNAs (15 μg of each) were denatured, electrophoresed in agarose-formaldehyde gels, and transferred to nylon membranes. The membranes were prehybridized with ExpressHyb (Clontech) for 1 h at 68°C and hybridized with a ^{32}P-labeled cyclin D1 probe diluted in ExpressHyb solution for 2 h at 45°C. The results were quantified by scanning autoradiograms.

Luciferase reporter assays. For luciferase reporter assays, cells were seeded the day before transfection at a density of 5×10^4 cells per well in 24-well plates. NIH 3T3 cells were transfected with 0.4 to 0.7 μg of a cyclin D1 luciferase reporter construct (pGL3-1748D1Luc; a gift of S. Cook) together with 0.25 to 0.35 μg of the indicated expression plasmids. RhoE-3T3 cells were transfected with 0.6 μg of an E2F-responsive luciferase reporter plasmid (pE2F-Luc; Clontech). The cells were harvested 48 h later in passive lysis buffer (Promega), and the luciferase activity was measured with a MicroBeta counter. Levels of reporter gene induction in transiently transfected cells were calculated by normalizing the luciferase levels to total *Renilla* luciferase levels. Results are presented as means ± standard deviations (SD) of data from three independent experiments, each of which was done in duplicate.

Biosynthetic labeling and immunoprecipitations. Serum-starved cells grown in 10-cm-diameter dishes were stimulated with serum (10% fetal calf serum [FCS]) for 6 h in complete DMEM followed by 1 h in methionine- and cysteine-free DMEM. The cells were then labeled for 30 min with 100 μCi of [^{35}S]methionine-cysteine (Redivue Promix [^{35}S] in vitro cell labeling mix; Amersham)/ml and chased for the indicated times in complete DMEM. The cells were harvested on ice in lysis buffer (50 mM Tris-HCl [pH 7.4], 150 mM NaCl, 1 mM EDTA, and 1% [vol/vol] Triton X-100, plus the protease and phosphatase inhibitors described above) and were clarified by centrifugation (10,000 × *g*). The supernatants (equalized for protein concentration) were precleared by an overnight incubation at 4°C with 30 μl of protein G-Sepharose (Amersham), and radioactivity levels in the supernatants were also measured to check that the levels of incorporated ^{35}S correlated with the protein concentration. Immunoprecipitations were carried out by incubating the cleared supernatants for 2 h at 4°C with 2 μg of anti-cyclin D1 antibody (sc-8396; Santa Cruz) and then for 1 h at 4°C with 15 μl of protein G-Sepharose (Amersham). Immunoprecipitates were then washed four times in lysis buffer and resuspended in Laemmli loading buffer. Immunoprecipitated proteins were run in SDS–12% polyacrylamide gels, and the incorporated radioactivity was detected with a phosphorimager (Bio-Rad) and quantitated with Quantity One software.

Focus formation assays. NIH 3T3 cells or RhoE-3T3 cells were seeded at a cell density of 2×10^5 cells per well in six-well plates the day before transfection. The cells were transfected with the indicated vectors in six-well plates in duplicate. After 24 h, the cells were transferred to 10-cm-diameter plates and the medium was substituted with 5% FCS-containing DMEM when the cells reached confluence (typically 2 to 3 days later). After 12 to 15 days, the cells were stained with 0.5% (wt/vol) crystal violet in 70% ethanol, and the numbers of foci with diameters of >1 mm were counted.

RESULTS

Establishment of stable cell lines that inducibly express RhoE. Our laboratory has previously shown that the microinjection of RhoE into MDCK cells induces stress fiber disassembly together with a stimulation of cell migration (13). Interestingly, when the RhoE protein was injected into MDCK cells, we observed a significant inhibition in DNA synthesis compared to control-injected cells, as assessed by BrdU incorporation (R. M. Guasch and A. J. Ridley, unpublished data). In order to investigate the effects of RhoE on the cell cycle, we decided to generate stable cell lines that are capable of expressing HA-tagged RhoE in an inducible manner. We used the previously described S2-6 cell line, an NIH 3T3 derivative (45), to generate RhoE-inducible cell lines in which HA-RhoE expression is repressed in the presence of tetracycline. The removal of tetracycline led to a rapid induction of HA-RhoE expression that reached maximal levels at 4 h (Fig. 1A) and then remained the same for at least 5 days (data not shown). A quantitative analysis indicated that the levels of HA-RhoE were approximately five- to sevenfold higher than those of endogenous RhoE (data not shown), and its expression was reversible, as the reintroduction of tetracycline to the medium led to the loss of HA-RhoE expression in ~35 h (data not shown). Importantly, HA-RhoE expression was almost undetectable in cells grown in the presence of tetracycline, even upon a prolonged exposure of the immunoblots (Fig. 1A).

RhoE expression transiently affects the actin cytoskeleton. To date, the only biological effects described for Rnd proteins are on the actin cytoskeleton. Transient RhoE and Rnd1 expression in different cell types induces stress fiber disassembly, a loss of focal adhesions, and cell rounding (13, 23). We therefore tested whether the induction of HA-RhoE expression in RhoE-3T3 fibroblasts would have the same effects. RhoE induced a dramatic loss of actin stress fibers within 6 h (Fig. 1B), together with a significant reduction in the number of focal adhesions, as indicated by the diffuse vinculin staining (Fig. 1C). However, a time course analysis of RhoE expression revealed that at longer time points, the cells recovered and reverted to normal levels of stress fibers and a spread phenotype indistinguishable from that of control cells, despite the high levels of HA-RhoE expression (Fig. 1D). Thus, the strong effects elicited by acute RhoE expression on the actin cytoskeleton are transient and disappear within hours in cells that express RhoE for longer periods of time.

RhoE blocks G_1 phase cell cycle progression. To assess if RhoE has any effects on the cell cycle, we first investigated whether long-term RhoE expression could affect the rate of cell growth. The induction of HA-RhoE expression (without tetracycline) completely blocked cell growth (Fig. 2A). Trypan blue staining and cell viability measurements showed that the reduction in cell growth was not due to an increase in cell death (data not shown), suggesting that RhoE expression inhibited cell proliferation, in accordance with our original observations with MDCK cells. This effect was specific, since cells expressing a RhoE mutant (N37RhoE) analogous to N27Rnd1 (23), which does not detectably bind GTP or affect stress fibers (K. Riento and A. J. Ridley, unpublished data), were not impaired at all in the ability to proliferate (Fig. 2A) and since the growth of the parental S2-6 cell line that we employed to generate RhoE-3T3 cells was not affected by tetracycline removal (data not shown).

In order to investigate whether RhoE inhibits cell proliferation, we performed a fluorescence-activated cell sorting (FACS) analysis of RhoE-3T3 cells grown in the presence or absence of tetracycline. The induction of RhoE expression led to the accumulation of cells in G_1 (Fig. 2B). Furthermore, quiescent RhoE-expressing cells failed to progress through the G_1/S transition when they were stimulated by serum to enter the cell cycle, in contrast to control cells (Fig. 2C). We confirmed these results by analyzing BrdU incorporation to determine the percentages of S-phase cells. Control cells showed a high percentage of S-phase entry (~75% BrdU positive) 20 h after serum stimulation. In contrast, RhoE expression strongly inhibited S-phase entry (~10% BrdU positive) (Fig. 2D). Altogether, these results suggest that RhoE inhibits cell proliferation primarily by preventing S-phase entry.

Neither ROCK nor RhoA inhibition mediates RhoE-induced cell cycle arrest. RhoE has been shown to prevent

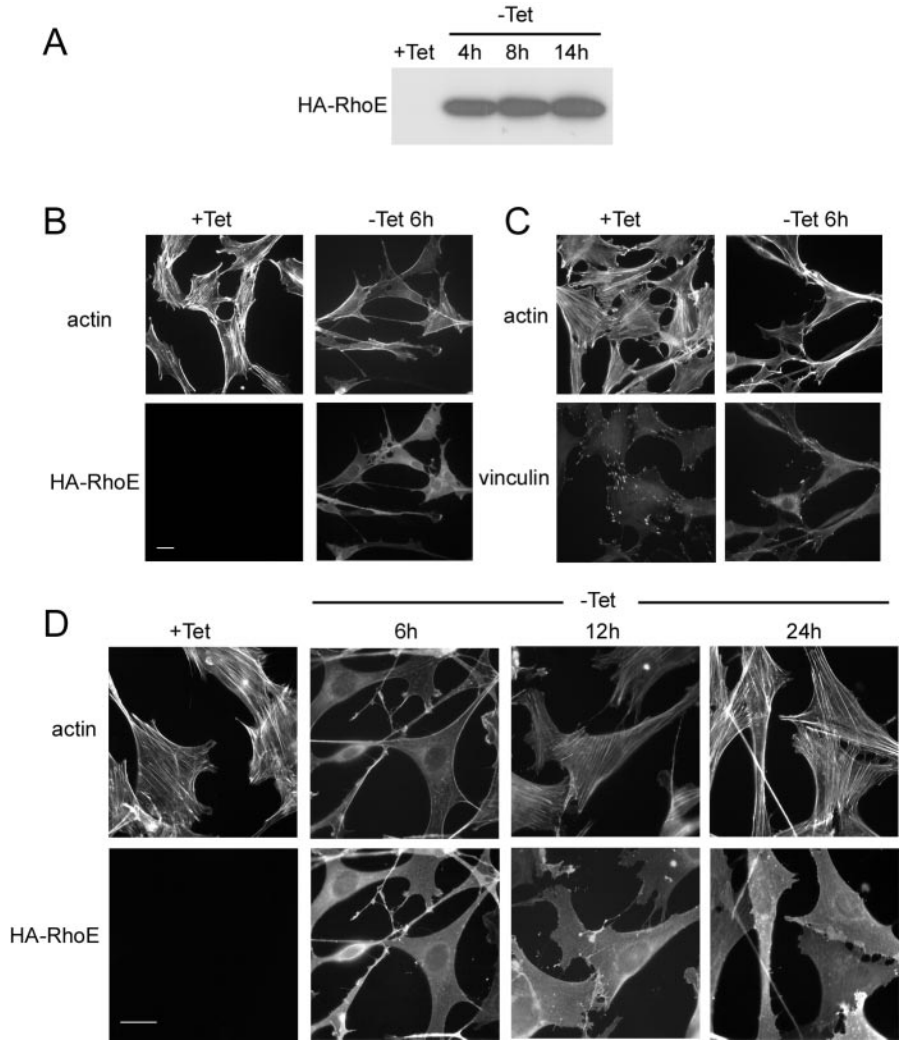

FIG. 1. Inducible expression of RhoE in RhoE-3T3 cells promotes loss of stress fibers and focal adhesions. RhoE-3T3 cells were grown in the presence (+Tet) or absence (−Tet) of tetracycline. (A) HA-RhoE expression following Tet removal was analyzed by Western blotting with an anti-HA antibody. (B) Fixed RhoE-3T3 cells were stained for F-actin and HA-RhoE with TRITC-labeled phalloidin and an anti-HA antibody, respectively. Bar, 5 μm. (C) Same as panel B, but the cells were stained for F-actin and vinculin with TRITC-labeled phalloidin and an antivinculin antibody, respectively. (D) RhoE-3T3 cells were fixed at the indicated time points after tetracycline removal and stained for F-actin and HA-RhoE with TRITC-labeled phalloidin and an anti-HA antibody, respectively. Bar, 5 μm. Similar results were obtained for three independent clones of RhoE-3T3 cells.

ROCK signaling, and thus stress fiber assembly, by binding directly to the N-terminal region of ROCK I (35). In addition, it has been reported that RhoE binding to p190RhoGAP stimulates its GAP activity towards RhoA, resulting in lower Rho-GTP levels and thus to a loss of stress fibers (49). We therefore investigated whether either of these mechanisms was involved in RhoE-induced cell cycle arrest. ROCK inhibition is not likely to be responsible for RhoE-mediated cell cycle arrest because cells treated with the ROCK inhibitor Y-27632 were not impaired in their proliferative ability (Fig. 3A), consistent with previously published observations (36, 39). In contrast, Rho inhibition is associated with cell cycle inhibition (48, 50). We therefore tested whether RhoE could modulate Rho-GTP levels in RhoE-3T3 cells. Pull-down experiments using GST-rhotekin indicated that HA-RhoE expression did not affect RhoA-GTP levels, either after HA-RhoE induction in growing cells (Fig. 3B) or in starved RhoE-expressing cells stimulated with serum to induce maximal RhoA activity (Fig. 3C). We also investigated whether constitutively active RhoA could rescue RhoE-induced cell cycle inhibition, using stably transfected RhoAV14-expressing RhoE-3T3 cells. Upon RhoE induction, cell growth was still inhibited in these cells, despite the expression of active RhoA (Fig. 3D). Altogether, these data suggest that neither ROCK nor RhoA inhibition, which is involved in RhoE-mediated stress fiber disassembly, accounts for RhoE-mediated cell cycle arrest.

RhoE prevents cyclin D1 and p21^{cip1} protein accumulation and E2F-regulated gene expression. In order to understand how RhoE inhibits G_1 phase progression, we analyzed the expression levels of different cell cycle regulators in RhoE-3T3 cells. Cyclin D1 peaked at mid-to-late G_1 (~9 h) in serum-stimulated control cells (Fig. 4A). In sharp contrast, cyclin D1

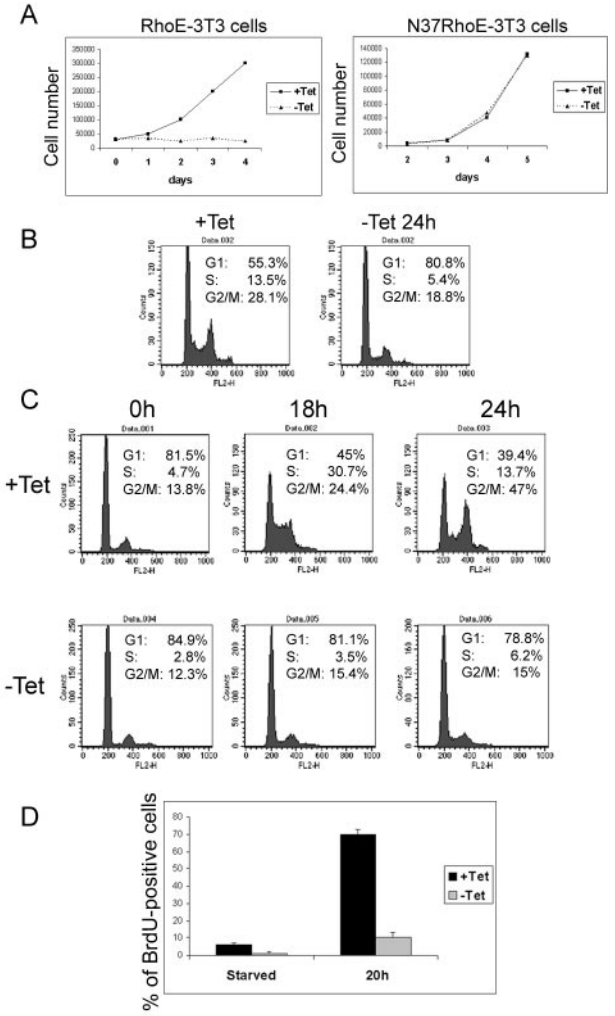

FIG. 2. RhoE blocks G_1-phase cell cycle progression. (A) RhoE-3T3 cells (left) or N37RhoE-3T3 cells (right) were plated and grown in the presence (+Tet) or absence (−Tet) of tetracycline, and cell growth was analyzed by counting the number of cells every 24 h. (B) RhoE-3T3 cells were grown in the presence or absence of tetracycline for 24 h and then harvested, and their DNA contents were analyzed by flow cytometry as described in Materials and Methods. (C) RhoE-3T3 cells were starved for 24 h in 0.5% FCS-containing medium in the presence or absence of tetracycline and then were stimulated with 10% FCS for the indicated times, harvested, and analyzed as for panel B. (D) RhoE-3T3 cells grown on coverslips were starved for 24 h in 0.5% FCS-containing medium in the presence or absence of tetracycline (starved) and were then stimulated with 10% FCS for 20 h in the presence or absence of tetracycline. Both starved and stimulated cells were incubated for the last 2 h with BrdU, fixed, and stained as described in Materials and Methods. The graph represents the mean values of BrdU-positive cells (calculated as percentages for >200 cells) from three independent experiments. The standard error for each value is shown. The data for panels A, B, and C are representative results from three independent experiments. The results shown in panel A were confirmed with two independently isolated clones of RhoE-3T3 cells and with a polyclonal (>50 clones) RhoE-3T3 cell population.

was almost undetectable in RhoE-expressing cells. A similar pattern was observed for $p21^{cip1}$, which was almost absent from RhoE-expressing cells. $p27^{kip1}$ was efficiently downregulated as control cells progressed through G_1 phase. However, although RhoE-expressing cells showed some downregulation of $p27^{kip1}$, they did not induce complete $p27^{kip1}$ degradation, probably as a consequence of their failure to progress into S phase. cdk4 and cdk2 levels were similar in control and RhoE-3T3 cells, and as expected, HA-RhoE was only present in tetracycline-deprived cells (Fig. 4A). Since G_1 progression ultimately leads to E2F activation via pocket protein phosphorylation, we analyzed the expression of two characterized E2F-dependent targets, p107 and cyclin A (20), as a readout of E2F activity and hence pocket protein inactivation. Whereas in control cells both proteins were induced in a cell cycle-dependent manner, their expression was almost undetectable in cells expressing RhoE at all time points analyzed (Fig. 4B). In concordance with these results, RhoE expression inhibited E2F transcriptional activity in a reporter gene assay using a luciferase-based

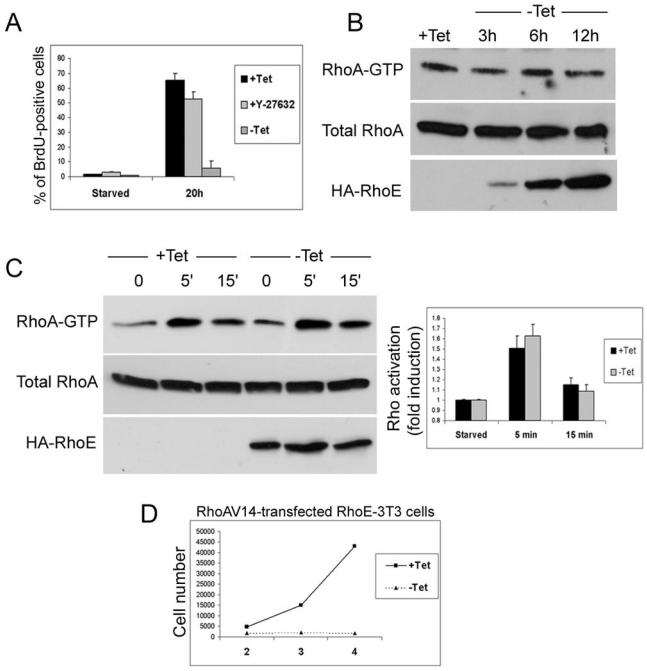

FIG. 3. Neither ROCK nor RhoA inhibition mediates RhoE-induced cell cycle arrest. (A) RhoE-3T3 cells grown on coverslips were starved for 24 h in 0.5% FCS-containing medium in the presence or absence of tetracycline (starved) and were then stimulated with 10% FCS for 20 h in the presence (+Tet) or absence (−Tet) of tetracycline or with 10 μM Y-27632 in the presence of tetracycline (+Y-27632). The cells were incubated for the last 2 h with BrdU, fixed, and stained as indicated in Materials and Methods. The graph represents the mean values of BrdU-positive cells (calculated as percentages for >200 cells) from three independent experiments. The standard error for each value is shown. (B) RhoE-3T3 cells were grown in the presence or absence of tetracycline and harvested at the indicated time points after tetracycline removal. RhoA activation was analyzed by GST-rhotekin pull-down followed by Western blotting with an anti-RhoA antibody (top). An aliquot of each lysate was also loaded in another gel to analyze total RhoA (middle) and HA-RhoE (bottom) protein levels. (C) Same as panel B, but the cells were starved for 24 h in 0.5% FCS-containing medium in the presence or absence of tetracycline and were then stimulated with 10% FCS and harvested at the indicated time points. The graph represents the quantified mean RhoA activation (Rho-GTP/total Rho) ± SD from three independent experiments. (D) RhoE-3T3 cells stably transfected with Flag-RhoAV14 were plated and grown in the presence (+Tet) or absence (−Tet) of tetracycline, and cell growth was analyzed by counting the number of cells every 24 h.

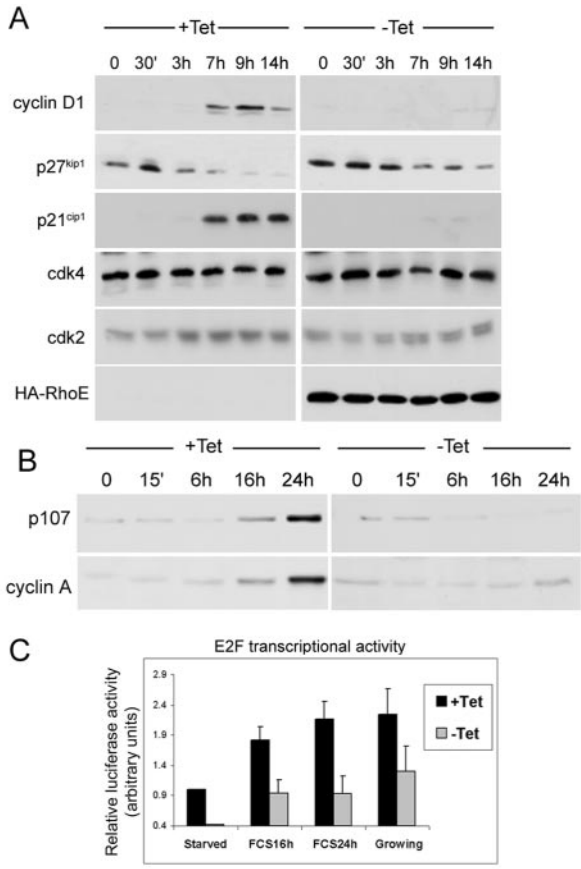

FIG. 4. RhoE prevents cyclin D1 and $p21^{cip1}$ protein expression and E2F-dependent transcription. (A) RhoE-3T3 cells were starved for 24 h in 0.5% FCS-containing medium in the presence (+Tet) or absence (−Tet) of tetracycline and were then stimulated with 10% FCS in the presence or absence of tetracycline and harvested at the indicated time points. The expression levels of cyclin D1, $p21^{cip1}$, $p27^{kip1}$, cdk4, cdk2, and HA-RhoE were analyzed by Western blotting with the indicated specific antibodies. (B) Same as panel A, but the expression levels of p107 and cyclin A were analyzed. (C) RhoE-3T3 cells were transiently transfected with the E2F luciferase reporter plasmid, grown for 48 h in the presence or absence of tetracycline (growing) or starved for 24 h in 0.5% FCS-containing medium (starved) in the presence or absence of tetracycline, and then stimulated with 10% FCS in the presence or absence of tetracycline for the indicated times. The cells were harvested, and luciferase activities were measured and represented as indicated in Materials and Methods.

reporter for E2F (Fig. 4C). Altogether, these results indicate that RhoE prevented the release of E2F from pocket proteins, an event induced by cdk phosphorylation. The lack of cyclin D1 protein in RhoE-expressing cells could therefore contribute to RhoE-induced G_1 arrest.

RhoE does not alter known signaling pathways upstream of cyclin D1 induction. We next focused on which signaling pathway promoting cyclin D1 expression might be affected by the expression of HA-RhoE. We first analyzed the activation levels of the ERK and phosphatidylinositide-3-kinase (PI3K)/Akt pathways in control and RhoE-3T3 cells, as they have been clearly implicated in cyclin D1 expression (37, 46). ERKs were transiently activated shortly after serum stimulation of control cells, and a very similar pattern of activation was observed for RhoE-expressing cells (Fig. 5A). Mid-G_1 expression of cyclin D1 has been shown to rely on sustained ERK activation, which is dependent on integrin clustering (38) and is regulated by ROCK (36). RhoE also did not affect the levels of phosphorylated focal adhesion kinase (FAK) (Fig. 5A), which has been shown to be involved in integrin-dependent cyclin D1 expression (51). PI3K pathway activation was monitored by analyzing the phosphorylation levels of two downstream effectors of this pathway that have been implicated in the regulation of cyclin D1 expression, specifically Akt and the forkhead family member FoxO3a (10, 41). Both Akt and FoxO3a were transiently phosphorylated in response to serum stimulation in both control and RhoE-expressing cells (Fig. 5A). Finally, we investigated the ability of RhoE-3T3 cells to induce Rac activation, since Rac has been shown to promote cyclin D1 expression (12, 16, 19). Rac was rapidly activated in both serum-stimulated control and RhoE-expressing cells, reaching a peak at 5 min and then declining back to basal levels (Fig. 5B). Thus, neither ERK, FAK, PI3K/Akt, nor Rac activation was impaired by RhoE expression, ruling out the possibility that RhoE blocked cyclin D1 induction due to an inhibition of any of these pathways.

RhoE blocks cyclin D1 expression at the posttranscriptional level. Since cyclin D1 expression can be regulated at multiple levels, we examined which level was affected in RhoE-expressing cells. Northern blotting revealed that the induction of cyclin D1 mRNA in response to serum stimulation was not inhibited by RhoE expression (Fig. 6A). We also investigated the ability of RhoE to modulate cyclin D1 promoter activity in luciferase-based reporter assays. RhoE cotransfection with the cyclin D1 promoter did not inhibit its transcriptional activity; on the contrary, RhoE slightly increased the cyclin D1 promoter's basal activity (Fig. 6B). Furthermore, RhoE did not inhibit RhoAV14-induced activation of the cyclin D1 promoter (Fig. 6B), although stable RhoAV14 expression in RhoE-expressing cells could not rescue cyclin D1 protein accumulation (data not shown). These results therefore suggest that RhoE expression does not impair the transcriptional induction of cyclin D1.

We next investigated whether RhoE could affect the accumulation of cyclin D1 at the protein level. Preventing cyclin D1 degradation with a proteasome inhibitor (aLLnL) led to an increase in the levels of cyclin D1 in RhoE-expressing cells, but this effect was more pronounced in control cells, suggesting that the rate of cyclin D1 synthesis is higher in control cells than in RhoE-expressing cells (Fig. 6C). In contrast, the degradation rate of cyclin D1 was similar regardless of the presence of RhoE, as revealed when cells were incubated with proteasome inhibitors to increase cyclin D1 levels and then were washed and exposed to cycloheximide to block de novo protein synthesis (Fig. 6D). These data point to an inhibitory effect of RhoE on cyclin D1 synthesis rather than to an increase in its degradation. To address this issue, we performed a pulse-chase analysis of cells that were metabolically labeled with [^{35}S]methionine-cysteine to investigate the rate of cyclin D1 synthesis and degradation. This showed that the biosynthesis of cyclin D1 was severely reduced in RhoE-expressing cells, but the degradation rate of the protein was not significantly affected upon RhoE expression (Fig. 6E).

RhoE-mediated cell cycle arrest requires pocket protein function. Since the absence of cyclin D1 probably prevents cyclin-dependent kinase activity and thus pocket protein hyperphos-

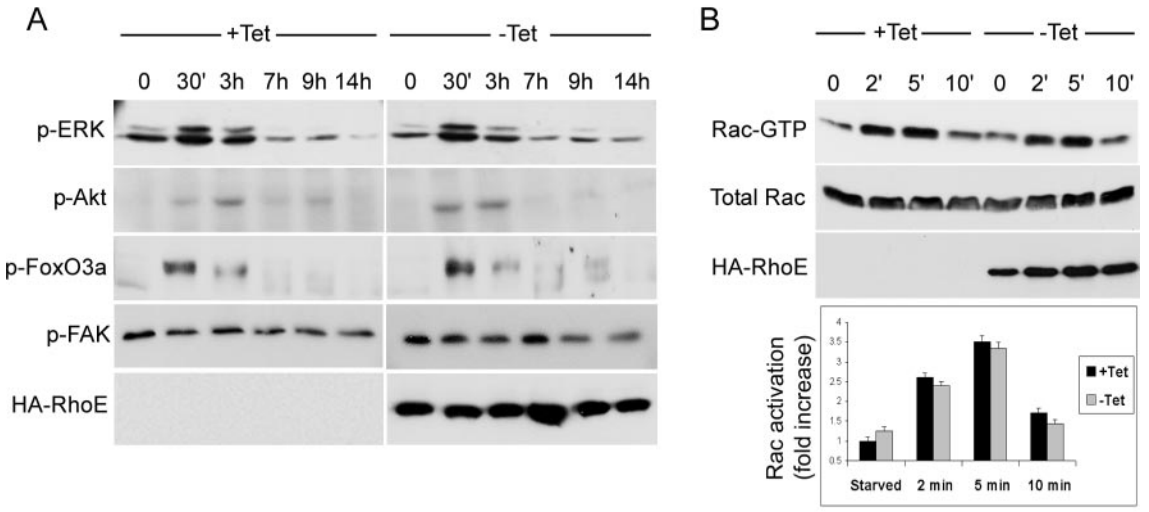

FIG. 5. RhoE does not alter signaling pathways upstream of cyclin D1 induction. (A) RhoE-3T3 cells were starved for 24 h in 0.5% FCS-containing medium in the presence (+Tet) or absence (−Tet) of tetracycline and were then stimulated with 10% FCS in the presence or absence of tetracycline and harvested at the indicated time points. The levels of phospho-ERK, phospho-Akt, phospho-FoxO3a, phospho-FAK, and HA-RhoE were analyzed by Western blotting with the indicated specific antibodies. (B) RhoE-3T3 cells were starved for 24 h in 0.5% FCS-containing medium in the presence (+Tet) or absence (−Tet) of tetracycline and were then stimulated with 10% FCS and harvested at the indicated time points. Rac activation was analyzed by a GST-PBD pull-down assay followed by Western blotting with an anti-Rac1 antibody (top). An aliquot of each lysate was also loaded in another gel to analyze total Rac (middle) and HA-RhoE (bottom) protein levels. The graph represents the quantified mean Rac activation (Rac-GTP/total Rac) and SD from three independent experiments.

phorylation, we analyzed whether enforced activation of the cdk-pRb axis could rescue cell cycle progression in RhoE-expressing cells. Interestingly, cyclin D1 expression alone was insufficient to rescue S-phase entry in RhoE-expressing cells, as shown in cell growth assays using cell lines stably expressing ectopic cyclin D1 (Fig. 7A) or by FACS analysis of transiently transfected cells (Fig. 7B). Very similar results were obtained with cells expressing a cyclin D1 construct fused to a p16-insensitive cdk4 point mutant (cdk4R24C) (30): both cell growth assays using cells stably expressing ectopic cyclin D1-cdk4R24C (Fig. 7A) and FACS analysis (Fig. 7C) showed that RhoE expression was still able to induce cell cycle arrest. However, the expression of human papillomavirus E7 or adenovirus E1A, which inhibits the function of the Rb family of pocket proteins, was able to rescue cell cycle progression in RhoE-3T3 cells, as indicated by growth curves of cells stably expressing E7 or E1A (Fig. 7A and C) and by FACS analysis of transiently transfected cells (Fig. 7B and C). Furthermore, the ectopic expression of cyclin E also rescued S-phase entry in RhoE-expressing cells (Fig. 7B), although to a lesser extent than E7 and E1A. These results indicate that RhoE requires functional pocket proteins to induce cell cycle arrest.

RhoE expression is increased in response to cisplatin. Since RhoE inhibits cell cycle progression in fibroblasts, we investigated whether endogenous RhoE levels changed upon stimulation with signals that affect cell proliferation. No significant changes in endogenous RhoE levels were observed when quiescent NIH 3T3 cells were stimulated with serum to induce cell cycle reentry (Fig. 8A). We next treated NIH 3T3 cells with a number of DNA-damaging agents in order to analyze RhoE expression in response to checkpoint induction. Interestingly, the treatment of cells with cisplatin induced an increase in endogenous RhoE levels that correlated with a decrease in cyclin D1 (Fig. 8B), suggesting that changes in RhoE levels may be relevant for cisplatin-mediated DNA damage-induced cell cycle arrest.

RhoE blocks Ras- and Raf-induced transformation. Since RhoE is able to inhibit cell cycle progression, as opposed to the growth-promoting role of RhoA, we reasoned that it might also have a negative role in cell transformation. Focus formation assays were performed with NIH 3T3 cells transfected with H-RasV12 and Raf-CAAX as positive controls to investigate the transforming potential of RhoE either alone or in combination with oncogenic Ras or Raf. As expected, both H-RasV12 and Raf-CAAX induced cell transformation, although Raf-CAAX had a weaker transforming potential than H-RasV12 (Fig. 9A). In sharp contrast, RhoE-transfected cells behaved the same as control transfected cells, failing to induce detectable foci. Interestingly, RhoE significantly inhibited both H-RasV12- and Raf-CAAX-induced cell transformation, correlating with its ability to block cell proliferation (Fig. 9A and B). Similarly, RhoE-3T3 cells expressing HA-RhoE (without tetracycline) were highly refractory to Ras-induced transformation, in contrast to control cells (Fig. 9C).

DISCUSSION

For this report, we have investigated the effects of RhoE on cellular responses by using RhoE-inducible cell lines. RhoE expression inhibited cell proliferation and induced a G_1 arrest, and it also reduced cell transformation by oncogenic Ras and Raf. Despite the activation of signaling pathways known to control cyclin D1 expression, RhoE-expressing cells failed to synthesize the cyclin D1 protein. The expression of E7, E1A, or cyclin E, which eliminates the Rb pocket protein G_1 checkpoint, was sufficient to rescue cell proliferation in RhoE-ex-

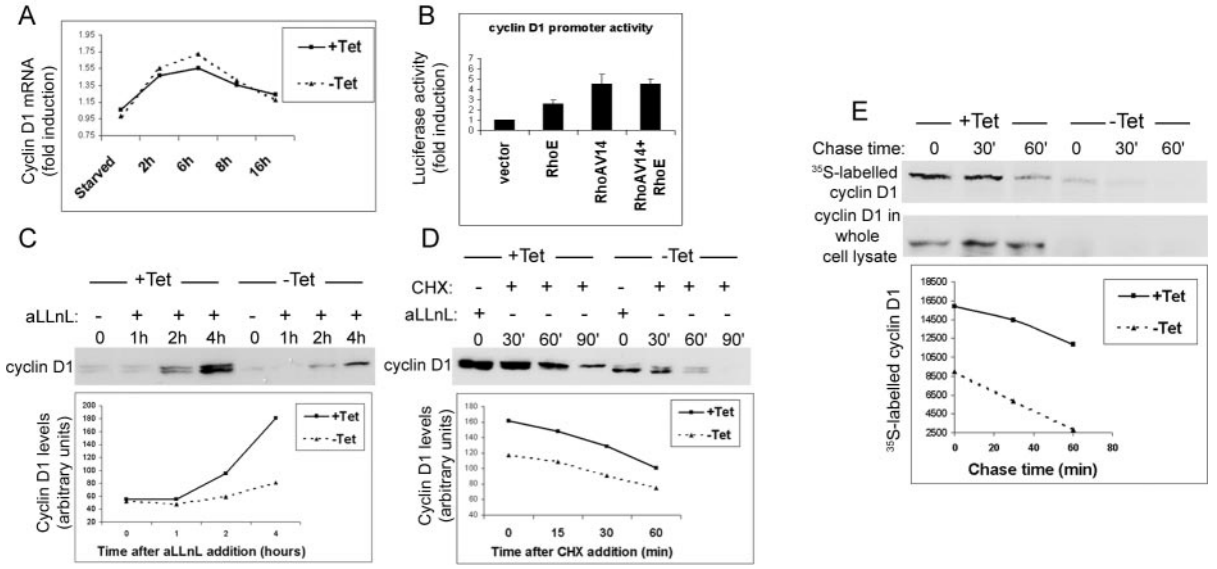

FIG. 6. RhoE blocks cyclin D1 expression at the posttranscriptional level. (A) RhoE-3T3 cells were starved for 24 h in 0.5% FCS-containing medium in the presence (+Tet) or absence (−Tet) of tetracycline and were then stimulated with 10% FCS in the presence or absence of tetracycline and harvested at the indicated time points. Cyclin D1 mRNA levels were analyzed by Northern blotting as indicated in Materials and Methods. Values were normalized for loading variations and expressed as fold induction over the amount of cyclin D1 mRNA present in starved cells. (B) NIH 3T3 cells were transiently transfected with the cyclin D1 promoter reporter construct together with the indicated expression vectors. Forty-eight hours after transfection, the cells were harvested and luciferase activities were measured and represented as indicated in Materials and Methods. (C) RhoE-3T3 cells grown in the presence (+Tet) or absence (−Tet) of tetracycline were incubated with 100 μM aLLnL (Sigma) and harvested at the indicated time points. The expression levels of cyclin D1 were analyzed by Western blotting with specific antibodies, quantified by image analysis, and represented in the adjacent graph. (D) RhoE-3T3 cells grown in the presence (+Tet) or absence (−Tet) of tetracycline were incubated for 4 h with 100 μM aLLnL, after which the medium was removed, the cells were washed, and medium containing 10 μg of cycloheximide (CHX)/ml was added. The cells were harvested at the indicated time points. The expression levels of cyclin D1 were analyzed by Western blotting with specific antibodies, quantified by image analysis, and represented in the adjacent graph. (E) RhoE-3T3 cells were starved for 24 h in 0.5% FCS-containing medium in the presence (+Tet) or absence (−Tet) of tetracycline and were then stimulated for 7 h with 10% FCS in the presence or absence of tetracycline. The cells were then pulse labeled with [^{35}S]methionine-cysteine for 30 min and harvested after the indicated chase times. Cyclin D1 was immunoprecipitated from the lysates as indicated in Materials and Methods. The graph represents the levels of radioactively labeled cyclin D1 measured by a phosphorimager and expressed in arbitrary units. All of the experiments shown in the figure were repeated three times with similar results.

pressing cells. Interestingly, endogenous RhoE levels increased in response to the DNA-damaging agent cisplatin, suggesting that RhoE could contribute to a checkpoint arrest induced by specific stimuli.

We consistently observed that RhoE inhibited cell growth, leading to the accumulation of RhoE-expressing cells in G_1, both in asynchronously growing cells and in synchronized cells. Cell cycle progression in fibroblasts requires cell attachment to the extracellular matrix via integrin-containing adhesions (42). Thus, the reduction in contractility and adhesion induced by RhoE could indirectly lead to cell cycle arrest, although ROCK-dependent stress fibers are not essential for cell proliferation (36). However, the cytoskeletal effects elicited by RhoE were only transient, since between 12 and 24 h after RhoE expression was first detected, normal levels of stress fibers were observed and the cell morphology was similar to that of control cells. It should be noted that previous work describing the cytoskeletal effects induced by Rnd family members analyzed cell morphology at short times after protein or cDNA injection (13, 23). Since our cell cycle analysis was performed long after RhoE-expressing cells had reverted to a normal cytoskeletal phenotype, cell cycle inhibition in response to RhoE was not a consequence of its cytoskeletal effects. In agreement with this, we found that long-term RhoE expression did not compromise signaling events that are sensitive to cytoskeletal alterations and/or adhesion defects, such as ERK and FAK activation (18, 52).

The most significant difference in G_1 regulators that we observed in RhoE-expressing cells was the lack of cyclin D1 and $p21^{cip1}$ expression. RhoE-expressing cells also did not fully downregulate $p27^{kip1}$ in response to serum, probably due to their failure to progress through the G_1/S transition, since $p27^{kip1}$ degradation is an event triggered by cdk2-dependent phosphorylation late in G_1 (47). The absence of $p21^{cip1}$ is not likely to compromise cell proliferation (8), but the lack of cyclin D1 in RhoE-expressing cells would prevent cdk4 activation and subsequent events in G_1 phase progression. cdk4 is one of the kinases that contribute to pocket protein phosphorylation and functional inactivation, and in agreement with this, RhoE-expressing cells showed a significant inhibition in E2F transcriptional activity, as indicated by reporter assays and by the reduced expression of known E2F target genes. Thus, activation of the G_1-phase regulatory machinery was impaired in RhoE-expressing cells.

Cyclin D1 serves as a major signaling integrator of G_1 progression, and its expression is tightly regulated by many signaling pathways, allowing extracellular signals to impinge on the core cell cycle machinery (9). Surprisingly, neither the ERK

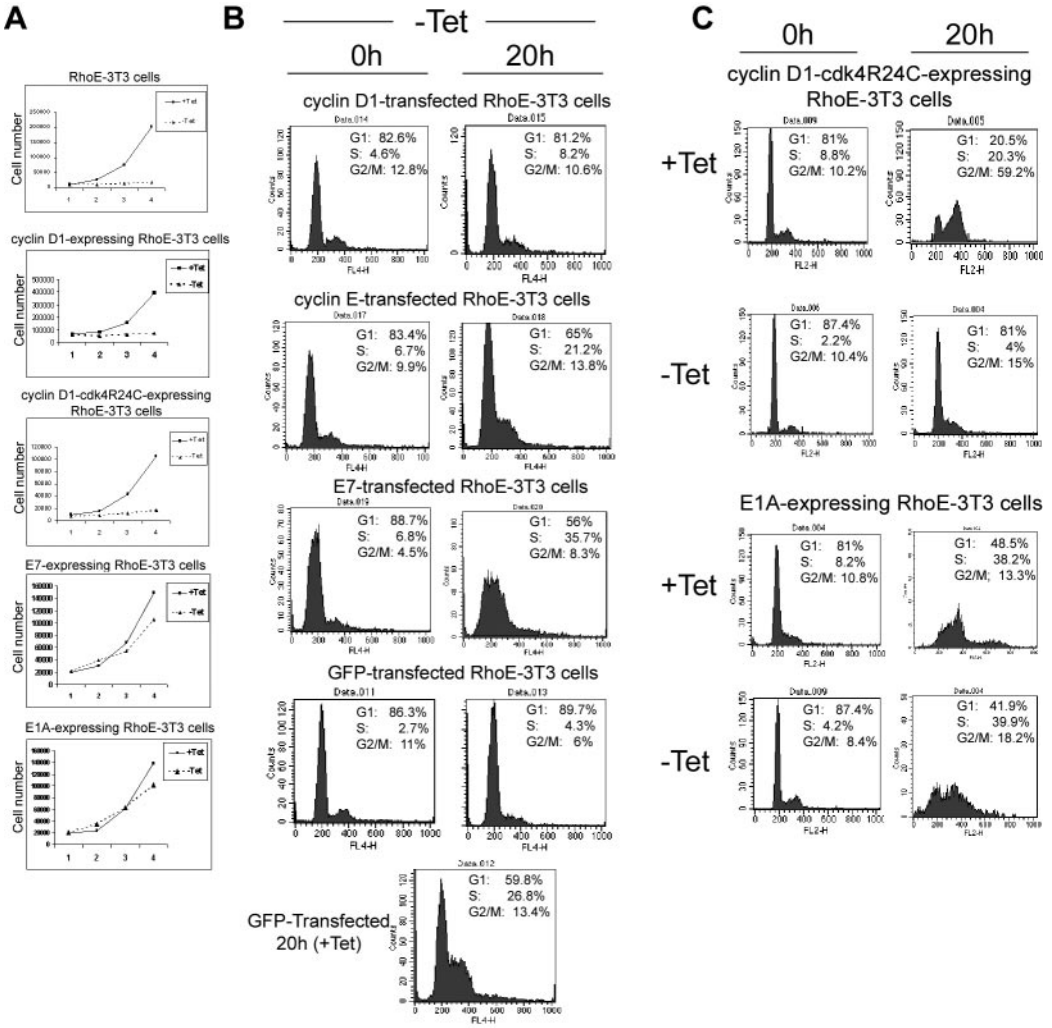

FIG. 7. RhoE-mediated cell cycle arrest is rescued by E7, E1A, and cyclin E. (A) RhoE-3T3 cells stably expressing the indicated vectors were plated and grown in the presence (+Tet) or absence (−Tet) of tetracycline, and cell growth was analyzed by counting the number of cells every 24 h. (B) RhoE-3T3 cells transiently transfected with the indicated vectors were starved for 24 h in 0.5% FCS-containing medium in the presence or absence of tetracycline, stimulated with 10% FCS for the indicated times, and then harvested. The DNA contents of the transfected cells were analyzed by flow cytometry as indicated in Materials and Methods. (C) RhoE-3T3 cells stably expressing the indicated vectors were starved for 24 h in 0.5% FCS-containing medium in the presence or absence of tetracycline, stimulated with 10% FCS for the indicated times, and then harvested. The DNA contents were analyzed by flow cytometry as indicated in Materials and Methods.

pathway nor the PI3K/Akt pathway, two major pathways that modulate cyclin D1 transcriptional activation (37, 46) and protein stability (10), appeared to be affected by RhoE. Similarly, we did not detect any differences in FAK and Rac activation, which have both been implicated in cyclin D1 expression (12, 51). It is possible that regulators further downstream on these pathways could be affected by RhoE. Interestingly, our data addressing the mechanisms underlying the lack of cyclin D1 showed that cyclin D1 transcriptional induction was not impaired by RhoE but that the production of cyclin D1 protein was inhibited.

Although the absence of cyclin D1 was the major alteration in the G_1-phase machinery that we observed in RhoE-expressing cells, ectopic expression of cyclin D1 alone could not rescue S-phase entry, indicating that RhoE probably affects multiple targets to induce cell cycle arrest. However, the observation that E7, E1A, and cyclin E were all able to promote cell proliferation in RhoE-expressing cells confirmed that RhoE-mediated G_1 arrest takes place prior to pocket protein hyperphosphorylation, as it can be overcome by signals that bypass the pRb-mediated restriction point.

We also analyzed changes in RhoE expression levels upon exposure to different stimuli in order to identify conditions in which RhoE could have a regulatory role in cell cycle progression. RhoE protein levels do not change throughout the cell cycle in NIH 3T3 cells, suggesting that RhoE does not regulate growth factor-induced cell cycle progression, although we cannot exclude the possibility that RhoE activity could be regulated through other mechanisms apart from altering expression levels. Interestingly, however, the induction of DNA damage with cisplatin, an antitumor agent that activates several checkpoint-related pathways leading to cell cycle arrest, induces an increase in RhoE levels. RhoE levels have also been reported to increase in response to UVB irradiation (21), suggesting

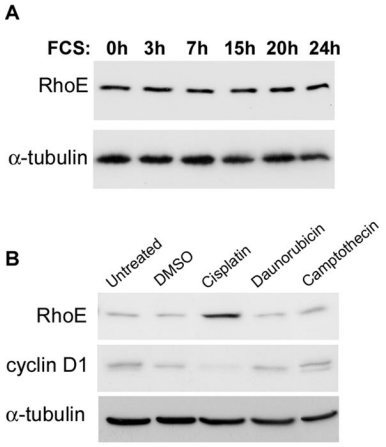

FIG. 8. RhoE expression is increased in response to cisplatin. (A) NIH 3T3 cells were starved for 24 h in 0.5% FCS-containing medium, stimulated with 10% FCS for the indicated times, and then harvested. The levels of RhoE and α-tubulin were then analyzed by Western blotting. (B) NIH 3T3 cells were treated for 24 h with 0.1% (vol/vol) dimethyl sulfoxide as a vehicle or with 10 μM cisplatin, 0.22 μM daunorubicin, or 4 μM camptothecin, and the levels of RhoE, cyclin D1, and α-tubulin were analyzed by Western blotting.

that RhoE may have a role in DNA damage-induced checkpoint control.

We also investigated whether the mechanisms that have been proposed to explain the cytoskeletal effects induced by RhoE, namely, ROCK I inhibition (35) and p190RhoGAP activation (49), could account for RhoE-mediated cell cycle arrest. The fact that RhoE induced cell cycle inhibition in the absence of visible cytoskeletal alterations suggests that the mechanisms underlying RhoE-induced cytoskeletal and proliferative effects could be independent. Since ROCK inhibition is compatible with cell proliferation (39), we reasoned that ROCK I inhibition did not account for the RhoE-mediated cell cycle inhibition. In contrast, RhoA inhibition is known to induce cell cycle arrest (40), and thus the RhoE-mediated effects on the cell cycle could be secondary to an inhibitory effect on RhoA. However, cell cycle inhibition induced by RhoA inhibition is characterized by different molecular events than RhoE-induced cell cycle arrest. Whereas RhoA (and ROCK) inhibition induces early cyclin D1 expression in NIH 3T3 cells (48), cyclin D1 levels are undetectable in RhoE-expressing NIH 3T3 cells. Moreover, cell cycle arrest induced by RhoA inhibition is linked to increases in $p21^{cip1}$ (25), whereas RhoE-expressing cells do not detectably express $p21^{cip1}$. Indeed, we did not detect any change in RhoA activation in RhoE-expressing cells, in contrast with a previous report (49) in which mouse embryo fibroblasts transduced with Tat-fused RhoE showed decreased RhoA-GTP levels. It is conceivable that the effects observed by Wennerberg et al. are transient and/or only apparent upon the expression of very high levels of RhoE. Importantly, RhoA activation is not affected by RhoE in the context of mitogen-induced cell cycle entry, indicating that RhoE-induced cell cycle arrest is independent of its reported effect on RhoA. Consistent with these observations, constitutively active RhoA could not rescue cell growth in RhoE-expressing cells.

The ability of RhoE to inhibit focus formation induced by oncogenes such as Ras and Raf is likely to be a consequence of inhibiting cell cycle progression. Interestingly, RhoE has been shown to be upregulated in colon cancer cell lines in response to sulindac, a nonsteroidal anti-inflammatory drug with antiproliferative properties in these cells. At the time, none of the identified cDNAs that were upregulated in response to sulindac provided a plausible explanation for its antiproliferative effects (1). Our data suggest that RhoE could contribute to the antiproliferative effects of nonsteroidal anti-inflammatory drugs. Conversely, estrogen treatment of prostatic stromal cells, a stimulus that has been implicated in prostate cancer progression, has been shown to induce RhoE repression, fueling the concept that RhoE may indeed have antitumoral effects (3). Although these data collectively suggest a negative role for RhoE in cell proliferation and transformation, RhoE can also enhance cell migration through its cytoskeletal effects (13) and

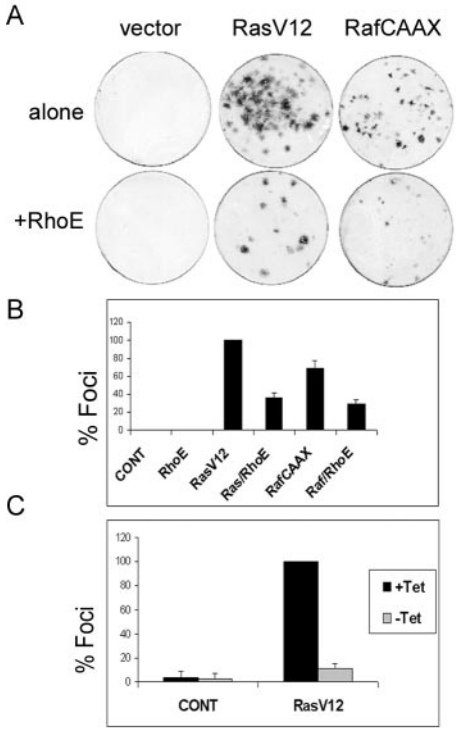

FIG. 9. RhoE blocks Ras- and Raf-induced transformation. (A) NIH 3T3 cells were transfected with the indicated expression plasmids and maintained in 5% serum for 12 to 15 days, with the medium replaced every 2 days. After 12 to 15 days, the cells were stained with crystal violet and the numbers of foci were counted. Shown are representative plates from a single experiment, conducted in duplicate. (B) Mean values from three independent experiments as described in panel A, each conducted in duplicate, are shown in the graph, representing the percentages of transformed foci relative to RasV12 transfectants. The standard error for each value is shown. (C) RhoE-3T3 cells were transfected with empty vector (control) or a RasV12 expression plasmid and maintained in 5% serum for 12 to 15 days, with the medium replaced every 2 days. During the last week, half of the plates were grown in the absence of tetracycline (−Tet). After 12 to 15 days, the cells were stained with crystal violet and the numbers of foci were counted. The mean values from three independent experiments, each conducted in duplicate, are shown in the graph, representing the percentages of transformed foci relative to RasV12 transfectants grown in the presence of tetracycline. The standard error for each value is shown.

could thereby contribute to cancer cell invasion. RhoE has indeed been shown to be important for morphological changes in the Raf-induced transformation of MDCK cells (14). RhoE may therefore have either a positive or a negative role in tumorigenesis, depending on the cellular background. Cancer cells harbor many oncogenic alterations, such as mutations in the cyclin D/p16/pRb axis, which deregulate their cell cycle machinery (43) and would override RhoE-imposed cell cycle arrest. These cells could benefit from a RhoE-mediated increase in invasiveness and motility. Interestingly, RhoE overexpression has been reported for a subclass of neuronal tumors, desmoplastic medulloblastomas (26).

In conclusion, we have shown that RhoE can inhibit cell proliferation and transformation in addition to its known effects on the actin cytoskeleton, and we propose that the fine-tuning of RhoE function in cells contributes to the balanced coordination of cell proliferation and migration.

ACKNOWLEDGMENTS

We are grateful to David G. Schatz for providing the S2-6 cell line and to Simon Cook, Julian Downward, Giles Cory, Roger Watson, Parmjit Jat, Carme Gallego, and Richard Marais for plasmids. We are also grateful to Ian Gerrard for technical assistance with FACS analysis and to Silvia Fernandez de Mattos for helpful advice on Northern blotting.

This work was supported by a BBSRC project grant (A.J.R) and an EMBO long-term postdoctoral fellowship (P.V.).

REFERENCES

1. **Akashi, H., H. J. Han, M. Iizaka, and Y. Nakamura.** 2000. Growth-suppressive effect of non-steroidal anti-inflammatory drugs on 11 colon-cancer cell lines and fluorescence differential display of genes whose expression is influenced by sulindac. Int. J. Cancer **88:**873–880.
2. **Assoian, R. K., and M. A. Schwartz.** 2001. Coordinate signaling by integrins and receptor tyrosine kinases in the regulation of G1 phase cell-cycle progression. Curr. Opin. Genet. Dev. **11:**48–53.
3. **Bektic, J., O. A. Wrulich, G. Dobler, K. Kofler, F. Ueberall, Z. Culig, G. Bartsch, and H. Klocker.** 2004. Identification of genes involved in estrogenic action in the human prostate using microarray analysis. Genomics **83:**34–44.
4. **Boyer, L., S. Travaglione, L. Falzano, N. C. Gauthier, M. R. Popoff, E. Lemichez, C. Fiorentini, and A. Fabbri.** 2003. Rac GTPase instructs NF-κB activation by conveying the SCF complex and IκBα to the ruffling membranes. Mol. Biol. Cell **15:**1124–1133.
5. **Bradford, M. M.** 1976. A rapid and sensitive method for the quantitation of microgram quantities of protein utilizing the principle of protein-dye binding. Anal. Biochem. **72:**248–254.
6. **Chardin, P.** 1999. Rnd proteins: a new family of Rho-related proteins that interfere with the assembly of filamentous actin structures and cell adhesion. Prog. Mol. Subcell. Biol. **22:**39–50.
7. **Clarke, N., N. Arenzana, T. Hai, A. Minden, and R. Prywes.** 1998. Epidermal growth factor induction of the c-*jun* promoter by a Rac pathway. Mol. Cell. Biol. **18:**1065–1073.
8. **Deng, C., P. Zhang, J. W. Harper, S. J. Elledge, and P. Leder.** 1995. Mice lacking p21CIP1/WAF1 undergo normal development, but are defective in G1 checkpoint control. Cell **82:**675–684.
9. **Diehl, J. A.** 2002. Cycling to cancer with cyclin D1. Cancer Biol. Ther. **1:** 226–231.
10. **Diehl, J. A., M. Cheng, M. F. Roussel, and C. J. Sherr.** 1998. Glycogen synthase kinase-3beta regulates cyclin D1 proteolysis and subcellular localization. Genes Dev. **12:**3499–3511.
11. **Etienne-Manneville, S., and A. Hall.** 2002. Rho GTPases in cell biology. Nature **420:**629–635.
12. **Gille, H., and J. Downward.** 1999. Multiple Ras effector pathways contribute to G_1 cell cycle progression. J. Biol. Chem. **274:**22033–22040.
13. **Guasch, R. M., P. Scambler, G. E. Jones, and A. J. Ridley.** 1998. RhoE regulates actin cytoskeleton organization and cell migration. Mol. Cell. Biol. **18:**4761–4771.
14. **Hansen, S. H., M. M. Zegers, M. Woodrow, P. Rodriguez-Viciana, P. Chardin, K. E. Mostov, and M. McMahon.** 2000. Induced expression of Rnd3 is associated with transformation of polarized epithelial cells by the Raf–MEK–extracellular signal-regulated kinase pathway. Mol. Cell. Biol. **20:** 9364–9375.
15. **Jaffe, A. B., and A. Hall.** 2002. Rho GTPases in transformation and metastasis. Adv. Cancer Res. **84:**57–80.
16. **Joyce, D., B. Bouzahzah, M. Fu, C. Albanese, M. D'Amico, J. Steer, J. U. Klein, R. J. Lee, J. E. Segall, J. K. Westwick, C. J. Der, and R. G. Pestell.** 1999. Integration of Rac-dependent regulation of cyclin D1 transcription through a nuclear factor-kappaB-dependent pathway. J. Biol. Chem. **274:** 25245–25249.
17. **Liberto, M., D. Cobrinik, and A. Minden.** 2002. Rho regulates $p21^{CIP1}$, cyclin D1, and checkpoint control in mammary epithelial cells. Oncogene **21:**1590–1599.
18. **Lipfert, L., B. Haimovich, M. D. Schaller, B. S. Cobb, J. T. Parsons, and J. S. Brugge.** 1992. Integrin-dependent phosphorylation and activation of the protein tyrosine kinase pp125FAK in platelets. J. Cell Biol. **119:**905–912.
19. **Mettouchi, A., S. Klein, W. Guo, M. Lopez-Lago, E. Lemichez, J. K. Westwick, and F. G. Giancotti.** 2001. Integrin-specific activation of Rac controls progression through the G_1 phase of the cell cycle. Mol. Cell **8:** 115–127.
20. **Muller, H., and K. Helin.** 2000. The E2F transcription factors: key regulators of cell proliferation. Biochim. Biophys. Acta **1470:**M1-M12.
21. **Murakami, T., M. Fujimoto, M. Ohtsuki, and H. Nakagawa.** 2001. Expression profiling of cancer-related genes in human keratinocytes following nonlethal ultraviolet B irradiation. J. Dermatol. Sci. **27:**121–129.
22. **Nobes, C. D., and A. Hall.** 1995. Rho, Rac, and Cdc42 GTPases regulate the assembly of multimolecular focal complexes associated with actin stress fibers, lamellipodia, and filopodia. Cell **81:**53–62.
23. **Nobes, C. D., I. Lauritzen, M. G. Mattei, S. Paris, A. Hall, and P. Chardin.** 1998. A new member of the Rho family, Rnd1, promotes disassembly of actin filament structures and loss of cell adhesion. J. Cell Biol. **141:**187–197.
24. **Olson, M. F., A. Ashworth, and A. Hall.** 1995. An essential role for Rho, Rac, and Cdc42 GTPases in cell cycle progression through G1. Science **269:** 1270–1272.
25. **Olson, M. F., H. F. Paterson, and C. J. Marshall.** 1998. Signals from Ras and Rho GTPases interact to regulate expression of p21Waf1/Cip1. Nature **394:** 295–299.
26. **Pomeroy, S. L., P. Tamayo, M. Gaasenbeek, L. M. Sturla, M. Angelo, M. E. McLaughlin, J. Y. Kim, L. C. Goumnerova, P. M. Black, C. Lau, J. C. Allen, D. Zagzag, J. M. Olson, T. Curran, C. Wetmore, J. A. Biegel, T. Poggio, S. Mukherjee, R. Rifkin, A. Califano, G. Stolovitzky, D. N. Louis, J. P. Mesirov, E. S. Lander, and T. R. Golub.** 2002. Prediction of central nervous system embryonal tumour outcome based on gene expression. Nature **415:**436–442.
27. **Qiu, R. G., A. Abo, F. McCormick, and M. Symons.** 1997. Cdc42 regulates anchorage-independent growth and is necessary for Ras transformation. Mol. Cell. Biol. **17:**3449–3458.
28. **Qiu, R. G., J. Chen, D. Kirn, F. McCormick, and M. Symons.** 1995. An essential role for Rac in Ras transformation. Nature **374:**457–459.
29. **Qiu, R. G., J. Chen, F. McCormick, and M. Symons.** 1995. A role for Rho in Ras transformation. Proc. Natl. Acad. Sci. USA **92:**11781–11785.
30. **Rao, R. N., N. B. Stamm, K. Otto, S. Kovacevic, S. A. Watkins, P. Rutherford, S. Lemke, K. Cocke, R. P. Beckmann, K. Houck, D. Johnson, and B. J. Skidmore.** 1999. Conditional transformation of rat embryo fibroblast cells by a cyclin D1-cdk4 fusion gene. Oncogene **18:**6343–6356.
31. **Ren, X. D., and M. A. Schwartz.** 2000. Determination of GTP loading on Rho. Methods Enzymol. **325:**264–272.
32. **Ridley, A. J.** 2001. Rho family proteins: coordinating cell responses. Trends Cell Biol. **11:**471–477.
33. **Ridley, A. J., and A. Hall.** 1992. The small GTP-binding protein Rho regulates the assembly of focal adhesions and actin stress fibers in response to growth factors. Cell **70:**389–399.
34. **Ridley, A. J., H. F. Paterson, C. L. Johnston, D. Diekmann, and A. Hall.** 1992. The small GTP-binding protein Rac regulates growth factor-induced membrane ruffling. Cell **70:**401–410.
35. **Riento, K., R. M. Guasch, R. Garg, B. Jin, and A. J. Ridley.** 2003. RhoE binds to ROCK I and inhibits downstream signaling. Mol. Cell. Biol. **23:** 4219–4229.
36. **Roovers, K., and R. K. Assoian.** 2003. Effects of Rho kinase and actin stress fibers on sustained extracellular signal-regulated kinase activity and activation of G_1-phase cyclin-dependent kinases. Mol. Cell. Biol. **23:**4283–4294.
37. **Roovers, K., and R. K. Assoian.** 2000. Integrating the MAP kinase signal into the G1 phase cell cycle machinery. Bioessays **22:**818–826.
38. **Roovers, K., G. Davey, X. Zhu, M. E. Bottazzi, and R. K. Assoian.** 1999. Alpha5beta1 integrin controls cyclin D1 expression by sustaining mitogen-activated protein kinase activity in growth factor-treated cells. Mol. Biol. Cell **10:**3197–3204.
39. **Sahai, E., T. Ishizaki, S. Narumiya, and R. Treisman.** 1999. Transformation mediated by RhoA requires activity of ROCK kinases. Curr. Biol. **9:**136–145.
40. **Sahai, E., and C. J. Marshall.** 2002. Rho-GTPases and cancer. Nat. Rev. Cancer **2:**133–142.
41. **Schmidt, M., S. Fernandez de Mattos, A. van der Horst, R. Klompmaker, G. J. Kops, E. W. Lam, B. M. Burgering, and R. H. Medema.** 2002. Cell cycle inhibition by FoxO forkhead transcription factors involves downregulation of cyclin D. Mol. Cell. Biol. **22:**7842–7852.
42. **Schwartz, M. A., and R. K. Assoian.** 2001. Integrins and cell proliferation: regulation of cyclin-dependent kinases via cytoplasmic signaling pathways. J. Cell Sci. **114:**2553–2560.

43. **Sherr, C. J.** 2000. Cell cycle control and cancer. Harvey Lect. **96:**73–92.
44. **Sherr, C. J., and J. M. Roberts.** 1999. CDK inhibitors: positive and negative regulators of G1-phase progression. Genes Dev. **13:**1501–1512.
45. **Shockett, P., M. Difilippantonio, N. Hellman, and D. G. Schatz.** 1995. A modified tetracycline-regulated system provides autoregulatory, inducible gene expression in cultured cells and transgenic mice. Proc. Natl. Acad. Sci. USA **92:**6522–6526.
46. **Takuwa, N., Y. Fukui, and Y. Takuwa.** 1999. Cyclin D1 expression mediated by phosphatidylinositol 3-kinase through mTOR-$p70^{S6K}$-independent signaling in growth factor-stimulated NIH 3T3 fibroblasts. Mol. Cell. Biol. **19:** 1346–1358.
47. **Vlach, J., S. Hennecke, and B. Amati.** 1997. Phosphorylation-dependent degradation of the cyclin-dependent kinase inhibitor p27. EMBO J. **16:** 5334–5344.
48. **Welsh, C. F., K. Roovers, J. Villanueva, Y. Liu, M. A. Schwartz, and R. K. Assoian.** 2001. Timing of cyclin D1 expression within G1 phase is controlled by Rho. Nat. Cell Biol. **3:**950–957.
49. **Wennerberg, K., M. A. Forget, S. M. Ellerbroek, W. T. Arthur, K. Burridge, J. Settleman, C. J. Der, and S. H. Hansen.** 2003. Rnd proteins function as RhoA antagonists by activating p190 RhoGAP. Curr. Biol. **13:**1106–1115.
50. **Yamamoto, M., N. Marui, T. Sakai, N. Morii, S. Kozaki, K. Ikai, S. Imamura, and S. Narumiya.** 1993. ADP-ribosylation of the rhoA gene product by botulinum C3 exoenzyme causes Swiss 3T3 cells to accumulate in the G1 phase of the cell cycle. Oncogene **8:**1449–1455.
51. **Zhao, J., R. Pestell, and J. L. Guan.** 2001. Transcriptional activation of cyclin D1 promoter by FAK contributes to cell cycle progression. Mol. Biol. Cell **12:**4066–4077.
52. **Zhu, X., and R. K. Assoian.** 1995. Integrin-dependent activation of MAP kinase: a link to shape-dependent cell proliferation. Mol. Biol. Cell **6:**273–282.